# Impedance of Electrochemical Cells

SPUR Final Paper, Summer 2012

Tianqi Wu
Mentor Yi Zeng
Project suggested by Yi Zeng

February 1, 2013

**Abstract**

In this study we studied the impedance of electrochemical cells, a characteristic property of such systems, for several one-dimensional and two-dimensional mathematical models, both analytically and numerically. In the 1D models we solved for the impedance, first under a simplifying assumption, and then exactly. We then used finite difference method to solve the 1D model numerically and confirmed the analytical results. Finally we formulated an isotropic 2D model, solved the resulting PDE using finite Hankel transform and Laplace transform, and found an asymptotic result of impedance which closely resembled the results from 1D model.

## 1 Introduction

Electrochemical cells are devices that generate voltage and current by chemical reactions, such as batteries or, inversely, drive chemical reactions when voltage and current is applied, such as electrolytic cells. The voltage correspond to the potential difference of the reactions, related by the Nernst equation, and the current correspond to the transfer of electrons due to the reactions. A particularly important type of electrochemical cells are fuel cells, which convert the chemical energy of a fuel into electricity through oxidation-reduction reactions, typically with oxygen; the most common fuel used is hydrogen.The difference between fuel cells and batteries is that fuel cells require constant input of fuel and oxygen and can run as long as the input is supplied. The general design of a fuel cell consists of an anode, a cathode, and electrolyte in between the two electrodes, with reactions occurring on the two electrode-electrolyte interfaces. The fuel is oxidized at the anode, and the positive ion formed moves through the electrolyte, which allows ions but not electrons to pass, while the free electron passes through the circuit connected to the fuel cell, creating a current in the circuit, before the two recombine at the cathode and react with another reactant, usually oxygen, to complete the process, producing water or carbon dioxide. There are many practical advantages of fuel cells over traditional energy technologies, such as low emission, high efficiency, fuel flexibility, durability, and scalability, and they have been used

for power in many applications, including commercial, industrial, and residential buildings and fuel cell vehicles that range from automobiles, airplanes, to submarines. [1]

Impedance is the measure of the total opposition to current generation in an alternating current system, defined as the complex ratio of voltage to current.[2] It is related to resistance, the measure of opposition to current generation in a direct current system, but is more general in that impedance includes not only opposition due to resistive effects, which gives resistance and forms the real part of impedance, but also opposition due to capacitive and inductive effects, which together form the imaginary part of impedance. The impedance of a system can be calculated by applying a small sinusoidal voltage input to the system and measuring the generated current signal; when this is done across a range of frequencies, the result is an impedance spectrum in response to frequency, usually depicted in a Nyquist plot, which shows the impedance spectrum on the complex plane, or in a Bode plot, which shows the magnitude of the impedance response against the frequency used. Two experimental technique for measuring the impedance are the galvanostatic intermittent titration technique (GITT) and the electrochemical impedance spectroscopy (EIS), also known as dielectric spectroscopy, now popularly used in characterizing electrode processes and interfaces, which can often reveal important information about them.[3][4]

In this paper, we study the impedance of electrochemical cells for one type of physical configuration, both analytically and numerically. The physical configuration in consideration is a very long cylindrical tube containing solutions of chemical species with chemical reactions occuring on one end of the tube, in which diffusion is the time-dominating effect. The paper is divided into the following sections. In section 1, we introduced the basic concepts and the objective of the study. In section 2, we formulate a long-term, one-dimensional mathematical model of the problem and solve for the impedance. In section 3, we remove the long-term assumption and solve the resulting PDE for the impedance, and compare its limiting behavior to the impedance from section 2. In section 4, we use the finite differece method to numerically solve the PDE, and compare the result with the analytical solution in section 3 using the Nyquist plot and the Bode plot. In section 5, we move on to an isotropic, two-dimensional mathematical model and solve for the impedance by applying the finite Hankel transform and the Laplace transform, and compare its limiting and asymptotic behavior with the previous models. In section 6, we discuss the results from the previous sections and possible directions of future research.

# 2 Results of Long-term 1D Model

We model the system as a very long container of solutions, with chemical reactions occurring at one end ($x = 0$). The baseline concentration of the system is $C_0$. After $t = 0$ a small external AC voltage $V(t) = V_0 e^{i\omega t}$ is applied at $x = 0$, which causes a concentration change $C(x, t)$ in the system and a current $I(t)$ at $x = 0$. Our goal is to compute the impedance $Z(t) = \frac{V(t)}{I(t)}$ of the system.

From the Nernst Equation

$$E = E^o - \frac{k_B T}{ne} \ln\left(\frac{\prod [\text{Products}]}{\prod [\text{Reactants}]}\right),$$

where $E$ is the cell potential, $E^o$ the standard cell potential, $k_B$ the Boltzmann constant, $T$ the temperature, $n$ the number of electrons transferred per reaction, and $e$ the charge of an electron, we get

$$V(t) = \frac{k_B T}{ne} \ln\left(\frac{C_0 + C(x=0,t)}{C_0}\right) \approx \frac{k_B T}{ne} \frac{C(x=0,t)}{C_0}. \tag{1}$$

The linear approxmiation holds because $V(t)$ is small, so $C(x=0,t)$ can be assumed to be negligible compared to $C_0$. In addition, we assume the reactions are quasi-equilibrium, i.e. no significant concentration change occurs internally, so we may take the total concentration to be $C_0 + C(x,t)$.

The current $I(t)$ is produced by the transfer of electrons during electrochemical reactions, so

$$I(t) = -neAF = -neAD\frac{\partial C}{\partial x}(x=0,t), \tag{2}$$

where $A$ is the cross-sectional area, $D$ the diffusitivity, and $F = D\frac{\partial C}{\partial x}(x=0,t)$ the flux of the species.

Since the system is large in lateral dimensions (y- and z-directions) relative to the scale of molecular diffusion, we may ignore boundary effects of y- and z-directions and assume concentration only varies in x-direction, and since the system is very long, we may assume it extends infinitely away from $x = 0$. Also, we assume the time-dominating effect in the system is the diffusion of one species, so other effects are negligible. Futhermore, we assume the diffusion is linear, so $D$ is independent of position and time, and for the purpose of simplifcation, we take $D$ to be constant. Under these assumptions,

$$\frac{\partial C}{\partial t}(x,t) = D\frac{\partial^2 C}{\partial x^2}(x,t). \tag{3}$$

Finally, since we are interested in the long-term behavior, we may assume $C(x,t)$ is separable, so

$$C(x,t) = C^*(x)e^{i\omega t}. \tag{4}$$

We solve for the impedance. Dividing 1 by 2, we get

$$Z(t) = \frac{V(t)}{I(t)} = \frac{k_B T}{(ne)^2 ADC_0} \frac{C(x=0,t)}{-\frac{\partial C}{\partial x}(x=0,t)} \tag{5}$$

Substituting 4 into 3, we get

$$i\omega C^*(x)e^{i\omega t} = De^{i\omega t}\frac{d^2 C}{dx^2}(x).$$

Cancelling $e^{i\omega t}$ on both sides, we get

$$i\omega C^*(x) = D\frac{d^2 C}{dx^2}(x).$$

Solving this ODE, we get

$$C^*(x) = C^*(0)e^{-\sqrt{\frac{i\omega}{D}}x}.$$

Plugging this back into 4, we get

$$C(x,t) = C^*(0)e^{-\sqrt{\frac{i\omega}{D}}x}e^{i\omega t}.$$

Differentiating this with respect to $x$ at $x = 0$, we get

$$\frac{\partial C}{\partial x}(x=0,t) = -\sqrt{\frac{i\omega}{D}}C(x=0,t).$$

Plugging this in 5, we get

$$Z(t) = \frac{k_BT}{(ne)^2ADC_0}\frac{C(x=0,t)}{-\frac{\partial C}{\partial x}(x=0,t)} = \frac{k_BT\sqrt{\frac{D}{i\omega}}}{(ne)^2ADC_0} = \frac{Z^*}{\sqrt{i\omega}}$$

where $Z^* = \frac{k_BT}{(ne)^2A\sqrt{D}C_0}$.

# 3 Analytical Results of 1D Model

The previous model is based on the long-term assumption 4, which we now remove. In this section we will solve the boundary value problem of the PDE 3 with the following initial and boundary conditions, from which we can compute the impedance using 5:

$$C(x=0,t) = ae^{i\omega t},$$

$$C(x>0,t=0) = 0,$$

$$C(x\to\infty,t) = 0,$$

where $a = \frac{neC_0V_0}{k_BT}$ from 1. These two are physically resonable, since initially the system is at baseline concentration and there is no concentration change, and the effect of concentration change due to voltage travels at a finite speed.

Let $W(x,t) = C(x,t) - ae^{i\omega t}$, then the original problem is transformed into

$$\begin{aligned} \frac{\partial W}{\partial t}(x,t) - D\frac{\partial^2 W}{\partial x^2}(x,t) &= -i\omega e^{i\omega t}, \\ W(x=0,t) &= 0, \\ W(x>0,t=0) &= -a. \end{aligned} \tag{6}$$

Furthermore, extend the x-domain to the whole x-axis, and extend the functions to odd functions on the whole line, i.e.

$$\frac{\partial W}{\partial t}(x,t) - D\frac{\partial^2 W}{\partial x^2}(x,t) = (-i\omega e^{i\omega t})\mathrm{sgn}(x). \tag{7}$$

$$W(x,t=0) = (-a)\mathrm{sgn}(x). \tag{8}$$

Once we solve $W$ in the extended problem above, its restriction to $0 < x < \infty$ would satisfy 6.

Note that the solution to the general boundary value problem

$$\frac{\partial W}{\partial t}(x,t) - D\frac{\partial^2 W}{\partial x^2}(x,t) = f(x,t).$$

$$W(x,0) = \phi(x).$$

is given by

$$W(x,t) = \int_{-\infty}^{\infty} S(x-y,t)\phi(y)dy + \int_0^t \int_{-\infty}^{\infty} S(x-y,t-s)f(y,s)dyds,$$

where

$$S(x,t) = \frac{e^{-\frac{x^2}{4Dt}}}{\sqrt{4Dt}\sqrt{\pi}}.$$

Plugging $f(x,t)$ and $\phi(x)$ from 7 and 8 in this, we get

$$W(x,t) = -a\int_{-\infty}^{\infty} S(x-y,t)\text{sgn}(y)dy + \int_0^t -i\omega a e^{i\omega s}ds \int_{-\infty}^{\infty} S(x-y,t-s)\text{sgn}(y)dy, \quad (9)$$

Note that

$$\int_{-\infty}^{\infty} S(x-y,t)\text{sgn}(y)dy = \int_0^{\infty} \left(S(x-y,t) - S(x+y,t)\right)dy.$$

Plugging in $S(x,t)$, we get

$$\int_{-\infty}^{\infty} S(x-y,t)\text{sgn}(y)dy = \int_0^{\infty} \left(\frac{e^{-\left(\frac{x-y}{\sqrt{4Dt}}\right)^2}}{\sqrt{4Dt}\sqrt{\pi}} - \frac{e^{-\left(\frac{x+y}{\sqrt{4Dt}}\right)^2}}{\sqrt{4Dt}\sqrt{\pi}}\right)dy.$$

Evaluating the integral, we get

$$\int_{-\infty}^{\infty} S(x-y,t)\text{sgn}(y)dy = \frac{2}{\sqrt{\pi}}\int_0^{\frac{x}{\sqrt{4Dt}}} e^{-z^2}dz = \text{erf}\left(\frac{x}{\sqrt{4Dt}}\right).$$

Using this, 9 gives

$$W(x,t) = (-a)\text{erf}\left(\frac{x}{\sqrt{4Dt}}\right) - i\omega a\int_0^t \text{erf}\left(\frac{x}{\sqrt{4D(t-s)}}\right)e^{i\omega s}ds.$$

Back to the original problem, we get

$$C(x,t) = W(x,t) + ae^{i\omega t} = a\left(e^{i\omega t} - \text{erf}\left(\frac{x}{\sqrt{4Dt}}\right) - i\omega\int_0^t \text{erf}\left(\frac{x}{\sqrt{4D(t-s)}}\right)e^{i\omega s}ds\right).$$

Differentiating this with respect to $x$ at $x = 0$, we get

$$\frac{\partial C}{\partial x}(x=0,t) = -\frac{a}{\sqrt{\pi D}}\left(\frac{1}{\sqrt{t}} + i\omega\int_0^t \frac{e^{i\omega s}}{\sqrt{t-s}}ds\right) = -\frac{a}{\sqrt{\pi D}}\left(\frac{1}{\sqrt{t}} + 2i\sqrt{\omega}e^{i\omega t}\int_0^{\sqrt{\omega t}} e^{-iz^2}dz\right).$$

Plugging this in 5, we get

$$Z(t) = \frac{k_B T}{(ne)^2 A D C_0} \frac{C(x=0,t)}{-\frac{\partial C}{\partial x}(x=0,t)} = \frac{k_B T}{(ne)^2 A \sqrt{D} C_0} \frac{e^{i\omega t}}{\frac{1}{\sqrt{\pi t}} + \frac{2}{\sqrt{\pi}} i\sqrt{\omega} e^{i\omega t} \int_0^{\sqrt{\omega t}} e^{-iz^2} dz}. \tag{10}$$

Note that

$$\int_0^\infty e^{-iz^2} dz = \frac{\sqrt{\pi}}{2\sqrt{i}}.$$

Using this, and taking $t \to \infty$, 10 gives

$$Z(t \to \infty) = \frac{k_B T}{(ne)^2 A \sqrt{D} C_0} \frac{e^{i\omega t}}{\frac{2}{\sqrt{\pi}} i\sqrt{\omega} e^{i\omega t} \frac{\sqrt{\pi}}{2\sqrt{i}}} = \frac{Z^*}{\sqrt{i\omega}},$$

where $Z^* = \frac{k_B T}{(ne)^2 A \sqrt{D} C_0}$, which agrees with the impedance from section 1. This agreement is expected, since in the long term ($t \to \infty$) there is no difference between the models in section 1 and section 2.

# 4 Numerical Results of 1D Model

We now solve the boundary value probelm in the last section numerically using the finite difference method. Note that for small $\Delta t$ and $\Delta x$, we have

$$\frac{\partial C}{\partial t}(x,t) \approx \frac{C(x,t+\Delta t) - C(x,t)}{\Delta t},$$

$$\frac{\partial C}{\partial x}(x,t) \approx \frac{C(x+\Delta x,t) - C(x,t)}{\Delta x},$$

$$\frac{\partial^2 C}{\partial x^2}(x,t) \approx \frac{C_x(x+\Delta x,t) - 2C_x(x,t) + C_x(x-\Delta x,t)}{(\Delta x)^2}.$$

Plugging these in 3 and 5, we get

$$C(x,t+\Delta t) \approx C(x,t) + \frac{D\Delta t}{(\Delta x)^2} \left( C(x+\Delta x,t) - 2C(x,t) + C(x-\Delta x,t) \right),$$

and

$$Z(t) \approx -\frac{k_B T \Delta x}{(ne)^2 A D C_0} \left( \frac{C(\Delta x,t)}{C(x=0,t)} - 1 \right)^{-1}$$

Let $\mathbf{C}$ be the matrix with $\mathbf{C}(i,j) = C((i-1)\Delta x, (j-1)\Delta t)$, and $\mathbf{Z}$ be the row vector with $\mathbf{Z}(j) = Z((j-1)\Delta t)$, then the above give

$$\mathbf{C}(\cdot, j+1) \approx (\mathbf{I} + \frac{D\Delta t}{(\Delta x)^2} \mathbf{L}) \mathbf{C}(\cdot, j), \tag{11}$$

$$\mathbf{Z}(j) \approx -\frac{k_B T \Delta x}{(ne)^2 A D C_0} \left( \frac{\mathbf{C}(2,j)}{\mathbf{C}(1,j)} - 1 \right)^{-1}, \tag{12}$$

where

$$\mathbf{L} = \begin{pmatrix} -2 & 1 & 0 & ... \\ 1 & -2 & 1 & ... \\ ... & & & \\ ... & 0 & 1 & -2 \end{pmatrix}$$

Applying 11 iteratively, we can numerically find the concentration over any range of position and time, recorded in $\mathbf{C}$, and then use 12 to find the corresponding impedance over time. To take care of the boundary condition, we adjust $\mathbf{C}(1, j+1)$ accordingly after $j$-th iteration. The results are displayed in the figures 1 and 2. The constants are set as follows: $D = 2$, $\Delta x = 10^{-3}$, $\Delta t = 10^{-7}$, and all others 1. The Nyquist plot, which plots the negative imaginary part against the real part of impedance as angular frequency varies, and the Bode plot, which plots the log of magnitude of impedance against the log of angular frequency, are displayed in figures 3 and 4. In both cases, the plot from numerical computation closely coincides with the plot of the limit impedance from the theoretical solution for higher angular frequencies. This is reasonable from the following scale analysis. From 3, we make the estimate

$$\frac{C}{t} = D\frac{C}{x^2},$$

which gives position scale

$$x \sim \sqrt{Dt}.$$

Since the system is oscillating with angular frequency $\omega$, the relevant time scale $t$ is the period $\frac{2\pi}{\omega}$. Plugging this in the above, we get

$$x \sim \sqrt{\frac{2\pi D}{\omega}}$$

For sufficiently high $\omega$, the position scale $x$ is very small compared to the length of the system used in the numerical computation, which approximates the semi-infinite theoretical solution very well, so the numerical plot and theoretical plot are close for such $\omega$.

# 5 Results of Isotropic 2D Model

In this section, we model the system as a very long cylinder of radius $R = 1$, with an external voltage $V(t) = V_0 e^{i\omega t}$ applied at the circular end $S$ ($r < 1$, $z = 0$) after $t = 0$, causing a concentration change $C(r, z, t)$ in the system and current $I(t)$ at $z = 0$. Note we drop the $\phi$ coordinate because the model is isotropic. We remove the 1D assumption since the radial dimension is small and so boundary effects are not negligible. We keep the other assumptions from the 1D model: the system is semi-infinitely long, the time-dominating effect is the diffusion of one species, diffusivity $D$ is constant, the voltage $V(t)$ is related to concentration change $C(r < 1, z = 0, t)$ by 1, and current is given by 2 in integral form,

$$I(t) = \int_S -neD\frac{\partial C}{\partial z}(r, z = 0, t)dA = -neAD\pi \int_0^1 \frac{\partial C}{\partial z}(r, z = 0, t) \cdot 2rdr,$$

which gives the impedance for this model,

$$Z(t) = \frac{V(t)}{I(t)} = \frac{k_B T}{(ne)^2 D C_0 \pi} \frac{C(r<1, z=0, t)}{-\int_0^1 \frac{\partial C}{\partial z}(r, z=0, t) \cdot 2r dr}. \tag{13}$$

In addition, to account for the boundary effects, we assume the cylindrical surface ($r = 1$) radiates at rate $h$ proportional to the concentration change. The boundary value problem for this model is

$$\frac{\partial C}{\partial t}(r, z, t) = D\nabla^2 C(r, z, t) = D\left(\frac{\partial^2 C}{\partial r^2} + \frac{1}{r}\frac{\partial C}{\partial r} + \frac{\partial^2 C}{\partial z^2}\right)(r, z, t),$$

with initial and boundary conditions

$$C(r, z, t=0) = 0,$$
$$\left(\frac{\partial C}{\partial r} + hC\right)(r=1, z, t) = 0,$$
$$C(r<1, z=0, t) = ae^{i\omega t},$$
$$C(r, z\to\infty, t) = 0,$$

where $a = \frac{neC_0V_0}{k_BT}$ from 1.

Let $J_k(x)$ be the $k$th-order Bessel function of the first kind; $\beta_n$ the $n$th positive root of the differential equation

$$hJ_0(x) + xJ_0'(x) = 0, \tag{14}$$

with $\beta_0 = 0$; and $W_n(z, t)$ the zeroth-order Hankel transform with respect to $r$ for $C(r, z, t)$, defined as

$$W_n(z, t) = H_0\{C(r, z, t), \beta_n\} = \lim_{\beta\to\beta_n} \int_0^1 rC(r, z, t)J_0(\beta r)dr, \tag{15}$$

with the inverse transform given by the Fourier-Bessel series

$$C(r, z, t) = 2W_0(z, t) + \sum_{n=1}^{\infty} \frac{2J_0(\beta_n r)}{(1 + \frac{h^2}{\beta_n^2})J_0(\beta_n)^2} W_n(z, t). \tag{16}$$

Note that

$$H_0\left\{\left(\frac{\partial^2 C}{\partial r^2} + \frac{1}{r}\frac{\partial C}{\partial r}\right)(r, z, t), \beta_n\right\} = -\beta_n^2 W_n(z, t) + \beta_n J_0(\beta_n)\left(\frac{\partial C}{\partial r} + hC\right)(r=1, z, t).$$

Apply the zeroth-order Hankel transform with respect to $r$. Using the property above, the PDE and the boundary condition $\left(\frac{\partial C}{\partial r} + hC\right)(r=1, z, t) = 0$ become

$$\frac{\partial W_n}{\partial t}(z, t) = D\left(-\beta_n^2 W_n(z, t) + \frac{\partial^2 W_n}{\partial z^2}(z, t)\right).$$

Using 15, the remaining initial and boundary conditions become

$$W_n(z, t=0) = 0,$$

$$W_n(z=0,t) = ae^{i\omega t} \lim_{\beta\to\beta_n} \int_0^1 rJ_0(\beta r)dr = \lim_{\beta\to\beta_n} \frac{J_1(\beta)}{\beta} ae^{i\omega t},$$
$$W_n(z\to\infty,t) = 0,$$

Let $V_{n,s}(z)$ be the Laplace transform for $W_n(z,t)$ with respect to $t$, defined as

$$V_{n,s}(z) = L\{W_n(z,t),s\} = \int_0^\infty W_n(z,t)e^{-st}dt \tag{17}$$

Note that

$$L\left\{\frac{\partial W_n}{\partial t}(z,t),s\right\} = sV_{n,s}(z) - W_n(z,t=0)$$

Apply the Laplace transform with respect to $t$. Using the property above and the initial condition $W_n(z,t=0)=0$, the PDE becomes

$$\left(\frac{s}{D}+\beta_n^2\right)V_{n,s}(z) = \frac{\partial^2 V_{n,s}}{\partial z^2}(z)$$

Using 17, the remaining boundary conditions become

$$V_{n,s}(z=0) = \lim_{\beta\to\beta_n} \frac{J_1(\beta)}{\beta} L\{ae^{i\omega t},s\},$$

$$V_{n,s}(z\to\infty) = 0$$

Solving this ODE, we get

$$V_{n,s}(z) = \lim_{\beta\to\beta_n} \frac{J_1(\beta)}{\beta} L\{ae^{i\omega t},s\}e^{-z\sqrt{\frac{s}{D}+\beta_n^2}}$$

Taking the inverse Laplace transform of $V_{n,s}(z)$ with respect to $s$ gives

$$W_n(z,t) = \lim_{\beta\to\beta_n} \frac{J_1(\beta)}{\beta} ae^{i\omega t} \int_0^t L^{-1}\left\{e^{-z\sqrt{\frac{s}{D}+\beta_n^2}},\tau\right\} e^{-i\omega\tau}d\tau.$$

Substituting this in 16 gives

$$C(r,z,t) = ae^{i\omega t}\int_0^t \left(L^{-1}\left\{e^{-z\sqrt{\frac{s}{D}}},\tau\right\} + \sum_{n=1}^\infty \frac{2J_0(\beta_n r)}{(1+\frac{h^2}{\beta_n^2})J_0(\beta_n)^2}\frac{J_1(\beta_n)}{\beta_n}\left\{e^{-z\sqrt{\frac{s}{D}+\beta_n^2}},\tau\right\}\right)e^{-i\omega\tau}d\tau,$$

where we used the fact that

$$\lim_{\beta\to 0}\frac{J_1(\beta)}{\beta} = \frac{1}{2}.$$

Differentiating this with respect to $z$ at $z=0$ gives

$$\frac{\partial C}{\partial z}(r,z=0,t) = -ae^{i\omega t}\int_0^t \left(L^{-1}\left\{\sqrt{\frac{s}{D}},\tau\right\} + \sum_{n=1}^\infty \frac{2J_0(\beta_n r)}{(1+\frac{h^2}{\beta_n^2})J_0(\beta_n)^2}\frac{J_1(\beta_n)}{\beta_n}L^{-1}\left\{\sqrt{\frac{s}{D}+\beta_n^2},\tau\right\}\right)e^{-i\omega\tau}d\tau,$$

and so

$$-\int_0^1 \frac{\partial C}{\partial z}(r, z=0, t)\cdot 2r dr = ae^{i\omega t}\int_0^t \left( L^{-1}\left\{\sqrt{\frac{s}{D}}, \tau\right\} + \sum_{n=1}^{\infty} \frac{4h^2}{\beta_n^2(h^2+\beta_n^2)} L^{-1}\left\{\sqrt{\frac{s}{D}+\beta_n^2}, \tau\right\}\right) e^{-i\omega\tau} d\tau,$$

where we used the defining equation 14 for $\beta_n$ and the fact that

$$J_0'(x) = -J_1(x).$$

Substituting this and the boundary condition $C(r<1, z=0, t) = ae^{i\omega t}$ in 13, we get

$$Z(t) = \frac{\frac{k_B T}{(ne)^2 D C_0 \pi}}{\int_0^t \left( L^{-1}\left\{\sqrt{\frac{s}{D}}, \tau\right\} + \sum_{n=1}^{\infty} \frac{4h^2}{\beta_n^2(h^2+\beta_n^2)} L^{-1}\left\{\sqrt{\frac{s}{D}+\beta_n^2}, \tau\right\}\right) e^{-i\omega\tau} d\tau}.$$

Taking $t \to \infty$, we get

$$Z(t\to\infty) = \frac{\frac{k_B T}{(ne)^2 D C_0 \pi}}{\sqrt{\frac{i\omega}{D}} + \sum_{n=1}^{\infty} \frac{4h^2\sqrt{\frac{i\omega}{D}+\beta_n^2}}{\beta_n^2(h^2+\beta_n^2)}}. \tag{18}$$

In particular, when $h = 0$, i.e. the cylindrical surface is impermeable, we get

$$Z(t\to\infty) = \frac{\frac{k_B T}{(ne)^2 D C_0 \pi}}{\sqrt{\frac{i\omega}{D}}} = \frac{Z^*}{\sqrt{i\omega}},$$

where $Z^* = \frac{k_B T}{(ne)^2 A\sqrt{D} C_0}$, which agrees with the 1D models. This is expected, since when the cylindrical surface is impermeable, there is no radial variation in concentration, which reduces the problem to the 1D models in sections 2 and 3. On the other hand, when $h \to \infty$, i.e. the cylindrical surface is always kept at the baseline concentration, we get

$$\lim_{h\to\infty} Z(t\to\infty) = \frac{\frac{k_B T}{(ne)^2 D C_0 \pi}}{\sqrt{\frac{i\omega}{D}} + \sum_{n=1}^{\infty} \frac{4\sqrt{\frac{i\omega}{D}+\beta_n^2}}{\beta_n^2}} = 0.$$

This is expected, since when the cylindrical surface is always kept at the baseline concentration, while the concentration fluctuates with a constant magnitude at the circular end, the variation in concentration at the circular end near the cylindrical surface approaches infinity, which means the current is infinite and so the impedance is zero.

Taking $\omega \to \infty$ in 18, we get

$$\lim_{\omega\to\infty} \frac{Z(t\to\infty)}{\sqrt{\frac{D}{i\omega}}} = \frac{\frac{k_B T}{(ne)^2 D C_0 \pi}}{1 + \sum_{n=1}^{\infty} \frac{4h^2}{\beta_n^2(h^2+\beta_n^2)}},$$

so asymptotically as a function of $\omega$,

$$Z(t\to\infty) \sim \frac{1}{1+\kappa(h)} \frac{Z^*}{\sqrt{i\omega}},$$

where $Z^* = \frac{k_B T}{(ne)^2 A\sqrt{D C_0}}$ and

$$\kappa(h) = \sum_{n=1}^{\infty} \frac{4h^2}{\beta_n^2(h^2+\beta_n^2)}.$$

Making the approximation $\beta_n \approx n\pi$,

$$\kappa(h) \approx \int_1^{\infty} \frac{4h^2}{(x\pi)^2(h^2+(x\pi)^2)}dx = \frac{4}{\pi^2} + \frac{4\tan^{-1}(\frac{\pi}{h}) - 2\pi}{\pi h} \leq \frac{4}{\pi^2}.$$

Compared to the 1D models in sections 2 and 3, this asymptotic impedance as a function of $\omega$ differs by a coefficient $\frac{1}{1+\kappa(h)}$, which is due to the additional radial variation in concentration, induced by the radiating boundary condition. Furthermore, from the approximation we see this coefficient is on the order of approximately $\frac{1}{1+\frac{4}{\pi^2}} = 0.7116....$

# 6 Discussion and Conclusion

In this paper, we studied the impedance of electrochemical cells, an important measure of such systems which can often reveal information about their reactions and structures, for different mathematical models using analytical and numerical methods. In section 1 we gave the background information of the paper and our goal in this study. In section 2 we introduced a long-term one-dimensional model and solved for the impedance from the resulting ODE. In section 3 we dropped the long-term assumption and completely solved the resulting PDE for the impedance and found its long-term limit to be the same as the answer in section 1. In section 4 we solved the PDE numerically using the finite difference method, and found that the concentration and impedance from the numerical solution agreed with those in the analytical solution, as the Nyquist plot and the Bode plot showed, and the agreement grows closer when frequency increases, which is predicted by a scale analysis. In section 5 we formulated an isotropic two-dimensional model and solved the resulting PDE using the finite Hankel transform and Laplace transform and obtained a formula for the impedance, and found its asymptotic long-term limit to be in a similar form as in the 1D models.

We found that, in the long term, the impedance response to frequency was

$$Z(t \to \infty) = \frac{Z^*}{\sqrt{i\omega}}$$

where $Z^* = \frac{k_B T}{(ne)^2 A\sqrt{D C_0}}$ in the two 1D models. We also found a similar asymptotic impedance in the isotropic 2D model

$$Z(t \to \infty) \sim \frac{1}{1+\kappa(h)} \frac{Z^*}{\sqrt{i\omega}}$$

which only differed from the 1D result by $\frac{1}{1+\kappa(h)}$, a coefficient on the order of approximately 0.7. The exact agreement between the results from the two 1D models were expected, since their formulation only differed in a separable assumption, which would not matter in the long term. The similarity between the results from the 1D models and the isotropic 2D model was reasonable, since in the special case $h = 0$ the 2D model simplified to the 1D model and

for $h > 0$ there was an additional effect due to the radial variation in concentration. The numerical methods confirmed the analytical results for the 1D models, especially for high frequencies.

For future research, we may want to solve the 2D model numerically and further study the analytical results from the 2D model, as well as generalizing the problem to other physical configurations. Another possiblility is to fit our mathematical result to experimental data and use it to determine important physical quantities such as diffusivity from the data.

# 7 Acknowledgment

Thanks to Yi Zeng and Professor Martin Z. Bazant, who mentored me on this project, and Professor Pavel Etingof and Dr. Slava Gerovitch, who supervisedthis project during the 2012 SPUR of the MIT Mathematics Department.

# References

R. S. Khurmi, R. S. Sedha. *Materials Science*. S. Chand & Company Ltd., 2010.

Electrical Impedance. *Encyclopedia Britannica*.

A. Lasia. *Electrochemical Impedance Spectroscopy and Its Applications, Modern Aspects of Electrochemistry*. Kluwer Academic/Plenum Publishers, New York, 1999, Vol. 32, p. 143-248.

Y. Zhu, C. Wang. Galvanostatic Intermittent Titration Technique for Phase-Transformation Electrodes. *Journal of Physical Chemistry C*, 2010, 114, 2830-28418.

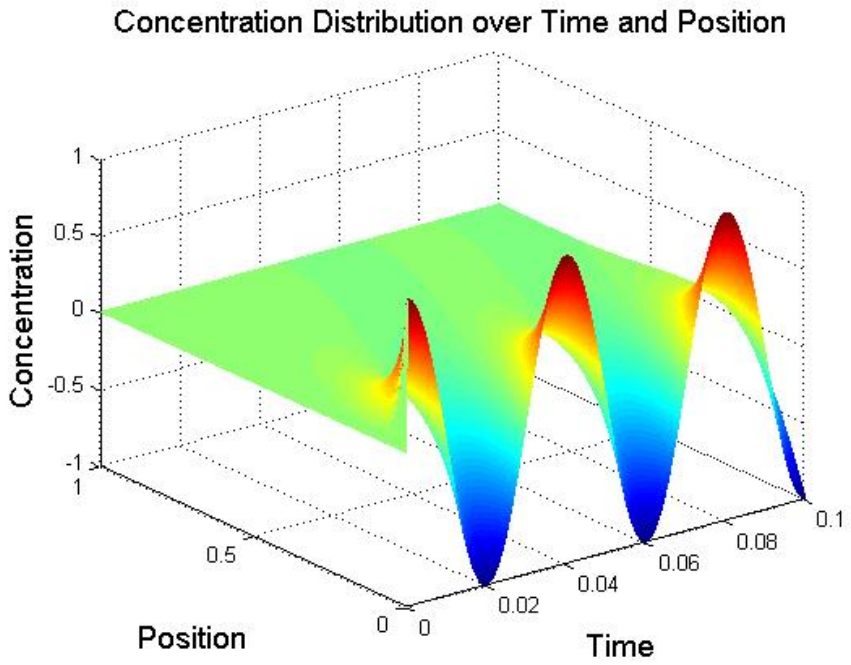


Figure 1: Concentration distribution, for 1000 positions from $x = 0$ to $x = 1$ and for 1000 times from $t = 0$ to $t = 0.1$, with input angular frequency $\omega = 50\pi$.

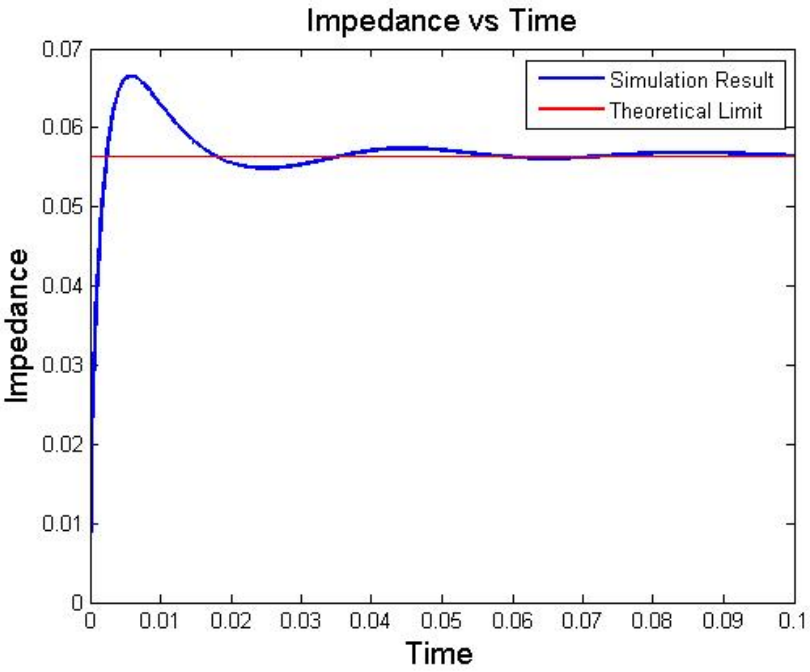


Figure 2: Magnitude of impedance, for 1000 times from $t = 0$ to $t = 0.1$, with input angular frequency $\omega = 50\pi$. Contrasted is the limit $|Z| = 0.056$ calculated from the theoretical solution.

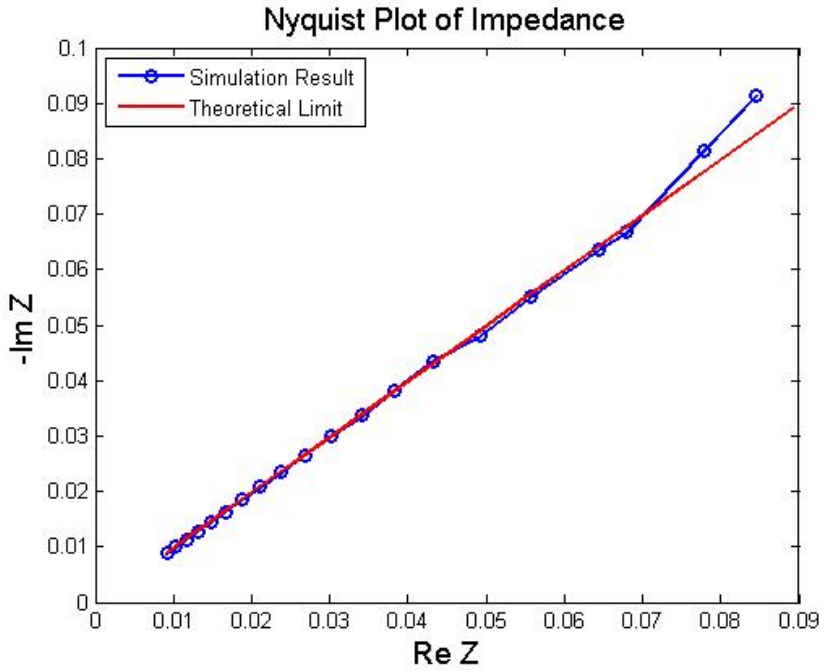


Figure 3: Nyquist plot of impedance at $t = 0.1$, for 20 input angular frequencies from $\omega = 10\pi$ to $\omega = 1000\pi$. Contrasted is the Nyquist plot of the limit impedance calculated from the theoretical solution, which is a line of slope 1. Note the two plots closely coincide for higher angular frequencies, which correspond to smaller values of $\mathrm{Re}(Z)$ and $-\mathrm{Im}(Z)$, i.e. lower left corner.

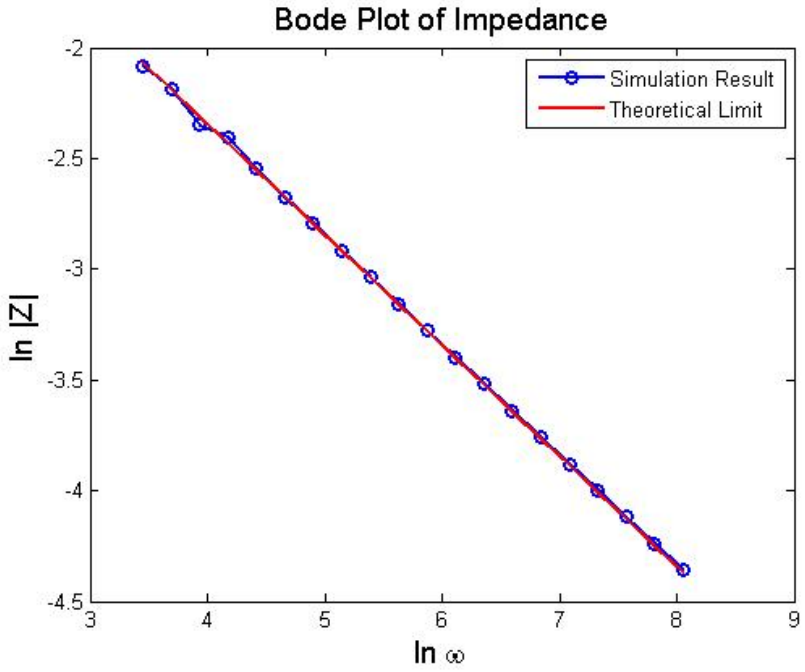


Figure 4: Bodet plot of impedance at $t = 0.1$, for 20 input angular frequencies from $\omega = 10\pi$ to $\omega = 1000\pi$. Contrasted is the Bode plot of the limit impedance calculated from the theoretical solution, which is a line of slope -1/2. Note the two plots closely coincide for higher angular frequencies, which correspond to smaller values of $\ln|Z|$, i.e. lower right corner.